Validation of H_2O continuum absorption models in the wave number range 180-600 cm^{-1} with atmospheric emitted spectral radiance measured at the Antarctica Dome-C site

Giuliano Liuzzi,[1] **Guido Masiello,**[1,2] **Carmine Serio,**[1,2,*]
Luca Palchetti,[3] **and Giovanni Bianchini**[3]

[1] *Scuola di Ingegneria, Universitá della Basilicata, 85100 Potenza, Italy*
[2] *CNISM, unitá di Ricerca di Potenza, Universitá della Basilicata, 85100 Potenza, Italy*
[3] *Istituto Nazionale di Ottica - CNR, largo E. Fermi 6, 50125 Firenze, Italy*

[*] *carmine.serio@unibas.it*

Abstract: This work presents the results concerning the analysis of a set of atmospheric emitted (down welling) spectral radiance observations in the spectral range 180 to 1100 cm^{-1} acquired at the Dome-C site in Antarctica during an extensive field campaign in 2011-2012. The work has been mainly focused on retrieving and validating the coefficients of the foreign contribution to the water vapour continuum absorption, within a spectral range overlapping the water vapour rotational band. Retrievals have been performed by using a simultaneous physical retrieval procedure for atmospheric and spectroscopic parameters. Both day (summer) and night (winter) spectra have been used in our analysis. This new set of observations in the far infrared range has allowed us to extend validation and verification of state-of-art water vapour continuum absorption models down to 180 cm^{-1}. Results show that discrepancies between measurements and models are less than 10% in the interval 350-590 cm^{-1}, while they are slightly larger at wave numbers below 350 cm^{-1}. On overall, our study shows a good consistency between observations and state-of-art models and provides evidence toward needing to adjust absorptive line strengths. Finally, it has been found that there is a good agreement between the coefficients retrieved using either summer or winter spectra, which are acquired in far different meteorological conditions.

OCIS codes: (300.6340) Spectroscopy, infrared; (030.5620) Radiative transfer; (280.4991) Passive remote sensing; (010.1280) Atmospheric composition.

References and links

1. S. A. Clough, M. J. Iacono, and J.-L. Moncet, "Line-by-line calculations of atmospheric fluxes and cooling rates: Application to water vapor," J. Geophys. Res. **97,** 15761–15785 (1992).
2. J. Harries, B. Carli, R. Rizzi, C. Serio, M. Mlynczak, L. Palchetti, T. Maestri, H. Brindley, and G. Masiello, "The farinfrared Earth," Rev. Geophys. **46,** RG4004 (2008).
3. S. A. Clough, F. X. Kneizys, and R. W. Davies, "Line shape and the water vapor continuum," Atmos. Res. **23,** 229–241 (1989).

#210874 - $15.00 USD Received 24 Apr 2014; revised 7 Jun 2014; accepted 7 Jun 2014; published 1 Jul 2014

4. D. C. Tobin, F. A. Best, P. D. Brown, S. A. Clough, R. G. Dedecker, R. G. Ellingson, R. K. Garcia, H. B. Howell, R. O. Knuteson, E. J. Mlawer, H. E. Revercomb, J. F. Short, P. F. W. van Delst, and V. P. Walden, "Downwelling spectral radiance observations at the SHEBA ice station: Water vapor continuum measurements from 17 to 6 mm," J. Geophys. Res. **104,** 2081–2092 (1999).
5. R. Bhawar, G. Bianchini, A. Bozzo, M. Cacciani, M. R. Calvello, M. Carlotti, F. Castagnoli, V. Cuomo, P. Di Girolamo, T. Di Iorio, L. Di Liberto, A. di Sarra, F. Esposito, G. Fiocco, D. Fuà, G. Grieco, T. Maestri, G. Masiello, G. Muscari, L. Palchetti, E. Papandrea, G. Pavese, R. Restieri, R. Rizzi, F. Romano, C. Serio, D. Summa, G. Todini, and E. Tosi, "Spectrally resolved observations of atmospheric emitted radiance in the H_2O rotation band," Geophys. Res. Lett. **35,** L04812 (2008).
6. C. Serio, F. Esposito, G. Masiello, G. Pavese, M. R. Calvello, G. Grieco, V. Cuomo, H. L. Buijs, and C. B. Roy, "Interferometer for ground-based observations of emitted spectral radiance from the troposphere: evaluation and retrieval performance," Appl. Opt. **47,** 3909–3919 (2008).
7. J. S. Delamere, S. A. Clough, V. H. Payne, E. J. Mlawer, D. D. Turner, and R. R. Gamache, "A far-infrared radiative closure study in the Arctic: Application to water vapor," J. Geophys. Res. **115,** D17106 (2010).
8. G. Masiello, C. Serio, F. Esposito, and L. Palchetti, "Validation of line and continuum spectroscopic parameters with measurements of atmospheric emitted spectral radiance from far to mid infrared wave number range," J. Quant. Spectrosc. Radiat. Transfer **113,** 1286–1299 (2012).
9. E. J. Mlawer, V. H. Payne, J.-L. Moncet, J. S. Delamere, M. J. Alvarado, and D. D. Tobin, "Development and recent evaluation of the MT_CKD model of continuum absorption," Phil. Trans. R. Soc. A **370,** 1–37 (2012).
10. P. D. Green, S. M. Newman, R. J. Beeby, J. E. Murray, J. C. Pickering, and J. E. Harries, "Recent advances in measurement of the water vapor continuum in the far-infrared spectral region," Phil. Trans. R. Soc. A **370,** 2637–2655 (2012).
11. C. Serio, G. Masiello, F. Esposito, P. Di Girolamo, T. Di Iorio, L. Palchetti, G. Bianchini, G. Muscari, G. Pavese, R. Rizzi, B. Carli, and V. Cuomo, "Retrieval of foreign-broadened water vapor continuum coefficients from emitted spectral radiance in the H_2O rotational band from 240 to 590 cm^{-1}," Opt. Express **16(20),** 15816–15833 (2008).
12. G. Bianchini and L. Palchetti, "Technical Note: REFIR-PAD level 1 data analysis and performance characterization," Atm. Chem. and Phys. **8,** 3817–3826 (2008).
13. R. Rizzi, L. Palchetti, B. Carli, R. Bonsignori, J. E. Harries, J. Leotin, S. C. Peskett, C. Serio, and A. Sutera, "Feasibility of the spaceborne radiation explorer in the far infrared (REFIR)," in *Optical Spectroscopic Techniques, Remote Sensing, and Instrumentation for Atmospheric and Space Research IV,* A. M. Larar and M. G. Mlynczak, eds., Proc. SPIE **4485,** 202 (2002).
14. L. Palchetti, G. Bianchini, F. Castagnoli, B. Carli, C. Serio, and F. Esposito, "Breadboard of a Fourier-transform spectrometer for the Radiation Explorer in the Far Infrared atmospheric mission," Appl. Opt. **44,** 2970–2979 (2005).
15. U. Amato, D. De Canditiis, and C. Serio, "Effect of apodization on the retrieval of geophysical parameters from Fourier-transform spectrometers," Appl. Opt. **37,** 6537–6543 (1998).
16. U. Amato, G. Masiello, C. Serio, and M. Viggiano, "The σ-IASI code for the calculation of infrared atmospheric radiance and its derivatives," Env. Model. & Software **17(7),** 651–667 (2002).
17. F. Hilton, R. Armante, R. August, C. Barnet, A. Bouchard, C. Camy-Peyret, V. Capelle, L. Clarisse, C. Clerbaux, P.F. Coheur, A. Collard, C. Crevoisier, G. Dufour, D. Edwards, F. Faijan, N., Fourrié, A. Gambacorta, M. Goldberg, V. Guidard, D. Hurtmans, S. Illingworth, N. Jacquinet-Husson, T. Kerzenmacher, D. Klaes, L. Lavanant, G. Masiello, M. Matricardi, A. McNally, S. Newman, E. Pavelin, S. Payan, E. Péquignot, S. Peyridieu, T Phulpin, J. Remedios, P. Schlüssel, C. Serio, L. Strow, C. Stubenrauch, J. Taylor, D. Tobin, W. Wolf, and D. Zhou, "Hyperspectral Earth Observation from IASI: four years of accomplishments," Bulletin of the American Meteorological Society **93,** 347–370 (2012).
18. G. Masiello, C. Serio, A. Carissimo, and G. Grieco, "Application of ϕ-IASI to IASI: retrieval products evaluation and radiative transfer consistency," Atm. Chem. and Phys. **9,** 8771–8783 (2009).
19. G. Masiello and C. Serio, "Simultaneous physical retrieval of surface emissivity spectrum and atmospheric parameters from infrared atmospheric sounder interferometer spectral radiances," Appl. Opt. **52,** 2428–2446 (2013).
20. G. Liuzzi, G. Masiello, C. Serio, S. Fonti, F. Mancarella, and T. L. Roush, "Search for Martian methane with TES data: development of a dedicated radiative transfer code: first results," in *Infrared Remote Sensing and Instrumentation XXI,* M. Strojnik Scholl and G. Páez, eds., Proc. SPIE **8867,** (SPIE, Bellingham, WA, 2013) 88670B (2013).
21. G. Masiello and C. Serio "An effective water vapor self-broadening scheme for look-up-table-based radiative transfer," in *Remote Sensing of Clouds and the Atmosphere VII,* K. P. Schaefer, O. Lado-Bordowsky, A. Comeron, and R. H. Picard, eds., Proc. SPIE **4882,** 52 (2003).
22. S. A. Clough, M. W. Shephard, E. J. Mlawer, J. S. Delamere, M. J. Iacono, K. Cady-Pereira, S. Boukabara, and P. D. Brown, "Atmospheric radiative transfer modeling: a summary of the AER codes, Short Communication," J. Quant. Spectrosc. Radiat. Transfer **91,** 233–244 (2005).
23. L. S. Rothman, I. E. Gordon, Y. Babikov, A. Barbe, D. Chris Benner, P. F. Bernath, M. Birk, L. Bizzocchi,

V. Boudon, L. R. Brown, A. Campargue, K. Chance, E. A. Cohen, L. H. Coudert, V. M. Devi, B. J. Drouin, A. Fayt, J.-M. Flaud, R. R. Gamache, J. J. Harrison, J.-M. Hartmann, C. Hill, J. T. Hodges, D. Jacquemart, A. Jolly, J. Lamouroux, R. J. Le Roy, G. Li, D. A. Long, O. M. Lyulin, C. J. Mackie, S. T. Massie, S. Mikhailenko, H. S. P. Müller, O. V. Naumenko, A. V. Nikitin, J. Orphal, V. Perevalov, A. Perrin, E. R. Polovtseva, C. Richard, M. A. H. Smith, E. Starikova, K. Sung, S. Tashkun, J. Tennyson, G. C. Toon, V. G. Tyuterev, and G. Wagner, "The HITRAN2012 molecular spectroscopic database," J. Quant. Spectrosc. Radiat. Transfer **130,** 4–50 (2013).

24. C. D. Rodgers, *Inverse Methods for Atmospheric Sounding Theory and Practice* **2** (World Scientific, Singapore, 2000).
25. A. Carissimo, I. De Feis, and C.Serio, "The physical retrieval methodology for IASI: the δ-IASI code," Env. Model. & Software **20(9),** 1111–1126 (2005).
26. G. Masiello, C. Serio, and P. Antonelli, "Inversion for atmospheric thermodynamical parameters of IASI data in the principal components space," Quantum J.R. Meteorol. Soc. **138,** 103-117 (2012).
27. P.-C. Hansen, "Analysis of Discrete Ill-Posed Problems by Means of the L-Curve," SIAM Review **34,** 561–580 (1992).
28. P. W. Rosenkranz, "Pressure broadening of rotational bands. II. Water Vapor from 300 to 1100 cm^{-1}," J. Chem. Phys. **87(1),** 163–170 (1987).
29. Q. Ma and R. H. Tipping, "The density matrix of H_2O-N_2 in the coordinate representation: A Monte Carlo calculation of the far-wing line shape," J. Chem. Phys. **112(3),** 574–584 (2000).

1. Introduction

The far infrared (FIR) emission of the Earth atmosphere includes H_2O transitions between pure rotational energy states, which significantly impact over atmospheric cooling rate and related climate processes and radiative forcing feedbacks. [1, 2].

Over the past years, the relatively unexplored FIR component of the spectrum, in contrast to the the better known midinfrared (MIR), has been the subject of various dedicated field measurement campaigns, which, in particular, have been capable to improve our knowledge and modeling accuracy of water vapour continuum absorption. In fact, with the advent and success of the Clough-Kneizys-Davies (CKD) empirical model [3] for the water vapour continuum and its latest development called MT-CKD [4], a number of experimental determinations of this absorption in the laboratory and the atmosphere have taken place. This has led to a series of validations and revisions to the empirical CKD and then MT-CKD model, noticeably at wave numbers greater than 350 cm^{-1}, while the lines and the associated continuum parameters at frequencies lower than 350 cm^{-1} are still now based uniquely on quantum-mechanical calculations.

The results obtained so far (see, e.g. [5–9]) show clearly that the MT-CKD model needs some further assessments, especially at wave numbers below 350 cm^{-1} [10].

The present work gives a quantitative validation of the most updated MT-CKD continuum model (version 2.5.2), against new down welling spectral radiance observations acquired at the Dome-C Antarctic station. The extremely dry climate of the site, particularly during the winter, allows us to investigate the spectroscopy of the water vapor rotational band at wave numbers that, in the case of the night (winter) spectra, are around 180 cm^{-1}. It is noteworthy that, to our knowledge, this is the first attempt of estimating the continuum coefficients in the full range 180-600 cm^{-1} using ground-based observations of atmospheric down welling spectral radiances. If we combine our, ground-based, results with those shown in [10], where the spectral range 85-410 cm^{-1} was explored with aircraft-based observations, we have now an experimental verification of the MT-CKD model in a very large portion of the water vapour rotational band, which can gain further confidence to the use of this model, e.g., for climate studies.

The retrieval of water vapour continuum coefficients has been performed with a novel methodology. This is an improvement based on an earlier method, which proved to be very effective to validate MT-CKD earlier version in the spectral range 350 to 600 cm^{-1} [8, 11]. In this new approach, the atmospheric parameters are simultaneously retrieved with those spectro-

scopic. Unlike the methodology shown in [8, 11] which was limited to retrieve bulk properties of atmospheric temperature and humidity, with the new approach spatial-vertically resolved profiles of atmospheric parameters (temperature and water vapour) are retrieved. This results in a procedure which allows us to check the consistency of spectroscopy, while zeroing the possible bias due to uncertainty associated with the thermodynamical state of atmosphere.

The present paper is organized as follows: section 2 will provide a full description of the instrumental setting and related data that have been analyzed; section 3 will deal with the inversion scheme and the forward model used to calculate synthetic spectra. Section 4 will describe the results obtained, giving particular emphasis to the continuum coefficient retrieval results and possible improvements.

2. Experimental

2.1. Brief outline of the Antarctic field campaign

The present work has been performed within the Italian PRANA (Proprietá Radiative del vapore Acqueo e delle Nuvole in Antartide - Radiative Properties of water vapour and clouds in Antarctica) project, which is mainly focused on providing an accurate characterization of the down welling FIR spectral radiance emitted from Earth's atmosphere in different sky conditions, with spectral measurements performed in a 2-year Antarctic field campaign. More extensively, the project is aimed to a better knowledge of the rotational water vapour band and radiative properties of high-altitude ice clouds, like cirrus and polar stratospheric clouds (PSC). The project started in December 2011 with the installation of the REFIR-PAD (Radiation Explorer in the Far InfraRed - Prototype for Applications and Development instrument [12]) spectrometer for the measurements of the downwelling radiance.

Although in this paper we will mostly focus on the analysis of REFIR-PAD data, there are several other instruments (Lidar systems, longwave/shortwave radiometers, daily radiosonde operations) at the measurement site which, as said, is located at Concordia Station, at Dome-C in Antarctica (75.10° S, 123.40° E, 3233 m asl). These instruments have been extensively used to characterize the state of the sky (clear/cloudy) in order to select appropriate REFIR-PAD spectra and to constrain the atmospheric state vector, when dealing with the inversion process of REFIR-PAD spectral radiances.

2.2. REFIR-PAD

The data used in this analysis have been acquired with the REFIR-PAD (from now on, simply REFIR), which is a portable Fourier Transform Spectrometer (FTS) operated with two uncooled pyroelectric detectors, and covering the nominal spectral range 100-1400 cm^{-1} with an unapodized resolution of 0.4 cm^{-1}. A summary of the main instrument specifications used during the Antarctic campaign is given in Table 1. The instrument was initially developed within the REFIR project [6, 13, 14], an European collaboration for the development of FIR instrumentation for a Space mission. For the Antarctic campaign, the instrument is installed inside a shelter devoted to atmospheric measurements and located in a clear area at about half kilometer from the main buildings of the station on the side which is windward in most days. The sky is observed at zenith direction through a roof aperture without any window in order to measure the down welling sky-view radiance without the window disturbance. The path between the roof aperture and the instrument is protected with an thermal isolated chimney to prevent cooling of the shelter interior.

The instrument is operated in continuous acquisition for 24 hours a day, alternating 6 hours of measurements to 3 hours of data analysis. The measurements are performed in cycles of about 12 minutes, which includes four acquisitions of the scene and four acquisitions of the reference internal blackbody sources for the radiometric calibration. For each acquisition, two spectra,

#210874 - $15.00 USD Received 24 Apr 2014; revised 7 Jun 2014; accepted 7 Jun 2014; published 1 Jul 2014

Table 1. REFIR-PAD instrument main specifications used in the Antarctic campaign.

Instrument type	Mach-Zehnder non polarising FTS
Beam splitter	Broadband Ge-coated Mylar
Operating spectral bandwidth	100-1400 cm^{-1}
Operating spectral resolution	0.4 cm^{-1} (unapodized, double-sided)
Optical throughput	0.01 cm^2 sr
Detector type	Room temperature pyroelectric (DLATGS)
Acquisition time	80 s per scan
Weight	55 kg (including control electronics)
Power consumption	50 W (24 VDC power supply)

one for each of the two output detectors, are recorded. Therefore, for each cycle of about 6 minutes of sky measurement, the final average spectrum of 8 spectra (four spectra times two detectors) is stored for the following data analysis. Furthermore, for each final spectrum an estimation of the noise is also calculated.

2.3. The data set of REFIR-PAD spectra

During the two years of the PRANA project, REFIR worked almost continuously recording about 40000 spectra of the sky under different meteorologic conditions.

For the current analysis, a first set of spectra have been selected which were recorded during the night of 9-10 February in between 21:00 to 02:00 UTC and a second set on 2 June 2012 between 14:00 UTC and 18:00 UTC.

Both data sets were acquired in atmospheric conditions characterized by a very low amount of precipitable water ranging from 0.15 mm to 1.15 mm; compare this to a humid tropical profile where the column water is typically about 40 mm. As it is possible to imagine, surface temperatures are extreme too, going from 245 K (-28 °C) for most of the summer spectra, to 200 K (-73 °C) for the coldest winter spectra. In this latter case, the air mass immediately above the ground is cooled down by the surface ice; this phenomenon, coupled with the absence of the solar heating, leads to a strong thermal inversion in the boundary layer, which is peculiar of most of the winter spectra.

In order to equalize the REFIR instrumental line shape [15], the selected spectra have been apodized with a Gaussian filter with a Half-Width at Half Maximum (HWHM) of 5/12 = 0.4167 cm^{-1}. It is important to stress that this apodization procedure does not affect the possibility to obtain a good estimation of the water vapour continuum, simply because the continuum absorption has a variability which is far lower than the HWHM of the Gaussian function used for apodization.

An example of REFIR spectrum is shown in Fig. 1 along with the radiometric noise of the instrument. It is clearly visible that the rotational water vapour band and the CO_2 ν_2 vibrational band are the dominant spectral features. The self-emission clearly visible in the core of the CO_2 absorption band is an effect not related to the air mass out of the instrument; in fact, because of the strong CO_2 absorption at 15 μm, the measured radiance at that wavelength corresponds just to the temperature of the environment close to the instrument. Among the lines of H_2O and CO_2, other minor features can be recognized, like the N_2O ν_2 band at 588.77 cm^{-1}, and the O_3 band centered at 1040 cm^{-1}. In principle REFIR is sensitive to the range 100 to 1400 cm^{-1}. However, for the present field campaign, problems of signal-to-noise ratio limits the useful range to 180-1100 cm^{-1}.

#210874 - $15.00 USD Received 24 Apr 2014; revised 7 Jun 2014; accepted 7 Jun 2014; published 1 Jul 2014

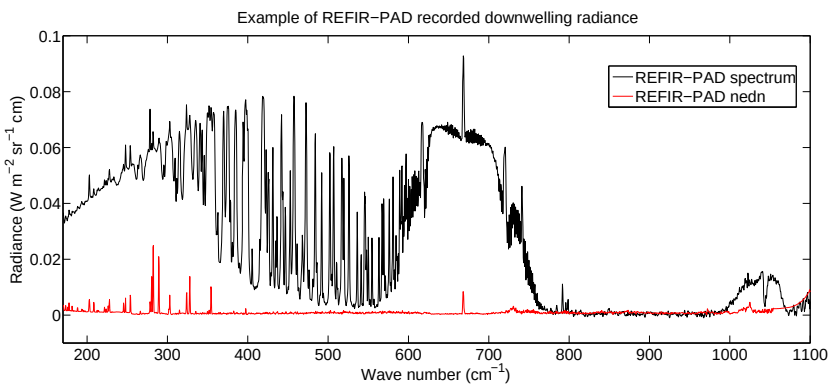

Fig. 1. Example of apodized REFIR spectrum, acquired at Dome-C on 20 January 2012, with a column of precipitable water vapour of 0.5 mm. The water vapour rotational band appears to be saturated below 240 cm^{-1}. Isolated spikes at the lower wave number range (visible in both spectrum and radiometric noise) are the effect of point calibration errors due to water vapour absorption (saturated water vapour lines) within the interferometers path. The same effect is seen at the center of the CO_2 most intense Q-Branch at 667 cm^{-1} which appears completely saturated.

3. Methods

3.1. Forward model

Forward calculations of REFIR spectra have been performed with the σ-IASI radiative transfer model [16], which has been originally conceived and developed for the IASI (Infrared Atmospheric Sounder Interferometer) instrument [17]. However, with minor changes, the code can be easily adapted to other optical interferometers/spectrometers with a spectral resolution in the range 0.1 to 2 cm^{-1}. The form of the radiative transfer equation, which σ-IASI considers in its numerical scheme, has been recently validated [18] and reviewed in [19, 20], which the interested reader is referred to. For the purpose of the present study, it is important to stress that σ-IASI is able to calculate both upwelling and downwelling spectral radiance, therefore it can be used to simulate ground-based observed radiances, as in this case. In addition to spectral radiance, the code also computes analytical Jacobian derivatives for atmospheric and spectroscopic parameters such as absorption coefficients of H_2O and CO_2 continua.

The σ-IASI code is a monochromatic radiative transfer code which uses a suitable look-up table for the monochromatic optical depth. In fact, the optical depth of a given atmospheric species is parameterized, layer by layer, by a low-order polynomial of the difference ΔT between the temperature T of that particular layer, and a reference layer temperature T_0. The polynomial coefficients are then stored in the look-up table, read by the program in order to perform the optical depths calculations. Unlike other gases, for water vapour, as one needs to take into account the self and foreign broadening effects of water vapor, the former of which depends on the water vapor concentration, a bi-dimensional look-up-table is used [21], which allows us to interpolate in two dimensions, that is, temperature and H_2O concentration.

For the present study, look-up tables have been developed using the optical depths computed with the most up-to-date available (at the time of the present study) version of LBLRTM (Line-by-Line Radiative Transfer Model) [22], release 12.2, with the line compilation AER (Atmospheric and Environmental Research) 3.2 and continuum model MT-CKD version 2.5.2. For the purpose of comparison, for water vapour, we have also used a look-up table directly derived from the H_2O line compilation available from HITRAN 2012 [23]. It is important to stress that

#210874 - $15.00 USD Received 24 Apr 2014; revised 7 Jun 2014; accepted 7 Jun 2014; published 1 Jul 2014

the look-up table for water vapour contains lines absorption, whereas the continuum absorption component is computed in such a way to be both in agreement with the CKD approach [3] and consistent with the given H_2O line compilation: either AER 3.2 or HITRAN 2012.

In mathematical terms, the appropriate water vapour absorption is generated according to the CKD approach [3], which states that the absorption coefficient of water vapour k at a specific wave number σ is the sum of a continuum term and of absorption due to all water vapour lines whose resonant frequency lies within 25 cm^{-1} to σ.

$$k = C_f \left(\frac{\rho_f}{\rho_o}\right) + C_s \left(\frac{\rho_s}{\rho_o}\right) + k_{local} \tag{1}$$

k_{local} is the contribution from all lines, each computed as the Lorentz line shape at σ minus the Lorentz line shape at 25 cm^{-1}. The continuum is composed of a foreign-broadened component C_f and a self-broadened C_s component, both expressed as cross sections (units of cm^2-molecule^{-1}). ρ_f and ρ_s are the densities of air and water vapour in molecules per cm^3. The parameter ρ_o is a reference broadener density defined as $\rho_o = P_o/(k_b T_o)$, where $P_o = 1013$ mbars, $T_o = 296$ K, and k_b is the Boltzmann constant.

In Earth's lower atmosphere, continuum absorption in spectral regions near the centers of water vapour bands is generally dominated by air-broadening, while window regions are dominated by self-broadening. Based on the MT-CKD model, for the spectral region 180 to 600 cm^{-1}, which we are interested in, and at altitudes and temperatures relevant to our experiment, the foreign to self absorption ratio steadily increases from 7 (at 600 cm^{-1}) to 70 and more (at 200 cm^{-1}). For this reason our analysis have focused on C_f alone, and within the inverse calculations we have performed to retrieve continuum coefficients, C_s was not adjusted.

The parameter C_f can be further decomposed in

$$C_f = \sigma \tanh\left(\frac{hc\sigma}{2k_b T}\right) C_f^o, \tag{2}$$

where σ is the wave number in cm^{-1}, h is the Planck constant, c is the speed of light, and T is the temperature. In this paper, we consider and show results about C_f^o. This will be referred in the following to as the continuum coefficients, and for the sake of a concise notation it will be denoted with c or $c(\sigma)$ when we will need to explicit its dependence on the wave number.

3.2. Retrieval methodology

The present paper is concerned with the simultaneous retrieval of continuum absorption coefficients and atmospheric parameters. We will not consider the retrieval of line parameters. However, the methodology is quite general and will be first presented without making any restriction on the composition of the retrieved state vector. Later in this section the approach will be specialized for our retrieval problem.

Let us assume that the inverse solution of the radiative transfer equation is sought through a Gauss-Newton iterative sequence. Then, without any loss of generality, let us assume that we are in a region around the first guess in which the problem is linear. If not, the scheme has to be further iterated according to the usual Gauss-Newton scheme. Remaining in the context of Rodgers' regularization [24], at a given step of the Gauss-Newton scheme, the estimate, $\mathbf{x}$ of atmospheric and spectroscopic parameters is obtained by solving the system of linear equations (e.g. [25, 26]),

$$(\gamma \mathbf{S}_a^{-1} + \mathbf{K}^t \mathbf{S}_\varepsilon^{-1} \mathbf{K})\mathbf{x} = \mathbf{K}^t \mathbf{S}_\varepsilon^{-1} \mathbf{y} + \gamma \mathbf{S}_a^{-1} \mathbf{x}_a \tag{3}$$

where $\mathbf{X}^t$ indicates the transpose of the generic variable $\mathbf{X}$, and $\mathbf{S}_\varepsilon, \mathbf{S}_a$ indicate the observational (measurement error) and a-priori covariance matrices, respectively. Here,

$$\mathbf{x} = \hat{\mathbf{v}} - \mathbf{v}_0; \quad \mathbf{x}_a = \mathbf{v}_a - \mathbf{v}_0; \quad \mathbf{y} = (\mathbf{R}_{obs} - \mathbf{R}_0) \tag{4}$$

#210874 - $15.00 USD Received 24 Apr 2014; revised 7 Jun 2014; accepted 7 Jun 2014; published 1 Jul 2014

where $\hat{\mathbf{v}}, \mathbf{v}_a, \mathbf{v}_0$ are the parameters state vector (to be estimated), the background vector and the first guess parameters state vector (the size of these vectors will be denoted with N). Moreover, $\mathbf{R}_{obs}$ is the observed radiance vector (whose size will be denoted with M), and $\mathbf{R}_0 = F(\mathbf{v}_0)$ with F the forward model function. Finally, the $M \times N$ derivative matrix or Jacobian, $\mathbf{K}$ is computed as

$$\mathbf{K} = \left.\frac{\partial F(\mathbf{v})}{\partial \mathbf{v}}\right|_{\mathbf{v}=\mathbf{v}_0}$$

The parameter γ in Eq. (3) is introduced in such a way to consider different optimization schemes for the final solution: $\gamma = 0$ corresponds to the unconstrained least squares minimization, $\gamma = 1$ to the usual Rodgers' regularization [24]. Furthermore, the parameter γ also helps to alleviate for possible forward model error (e.g., [26]). A suitable value for γ can be also chosen by the user, e.g., in the direction in which the χ^2-constraint decreases. In addition, objective selection could be obtained using, e.g., the so-called L-curve criterion [27]. With the L-curve approach, the philosophy is to try to minimize the root mean square error $E\left((\mathbf{x}_{true} - \mathbf{x})^2\right)$, where $E(\cdot)$ means expectation value. In the present work, an optimal value γ_{opt} of γ is obtained through the L-curve criterion, so that the explicit solution of system of equations 3 reads

$$\mathbf{x} = \left(\gamma_{opt}\mathbf{S}_a^{-1} + \mathbf{K}^t\mathbf{S}_\varepsilon^{-1}\mathbf{K}\right)^{-1}\left(\mathbf{K}^t\mathbf{S}_\varepsilon^{-1}\mathbf{y} + \gamma_{opt}\mathbf{S}_a^{-1}\mathbf{x}_a\right) \tag{5}$$

Under the usual assumption that the observations are not correlated with the background state, we derive for the a-posteriori covariance matrix of the final estimate, $\hat{\mathbf{v}}$ the expression shown below

$$\mathbf{S}_v = \mathbf{A}^{-1}\left(\gamma_{opt}^2\mathbf{S}_a^{-1} + \mathbf{K}^t\mathbf{S}_\varepsilon^{-1}\mathbf{K}\right)\mathbf{A}^{-1} \tag{6}$$

with

$$\mathbf{A} = \left(\gamma_{opt}\mathbf{S}_a^{-1} + \mathbf{K}^t\mathbf{S}_\varepsilon^{-1}\mathbf{K}\right) \tag{7}$$

which for $\gamma_{opt} = 1$ reduces to the usual form of the a-posteriori matrix for Rodgers' regularization [24]. An additional useful formula, which will be used later in this paper, expresses the sensitivity of the the retrieved state vector to any generic interfering set of parameters, say $\mathbf{x}_I$. The formula reads (e.g., [25])

$$\frac{\partial \mathbf{x}}{\partial \mathbf{x}_I} = \left(\gamma_{opt}\mathbf{S}_a^{-1} + \mathbf{K}^t\mathbf{S}_\varepsilon^{-1}\mathbf{K}\right)^{-1}\left(\mathbf{K}^t\mathbf{S}_\varepsilon^{-1}\mathbf{K}_I\right) \tag{8}$$

where $\mathbf{K}_I$ is the Jacobian derivative of $\mathbf{x}_I$. Equation (8) allows us to justify the claim we did at the end of section 3.1 that the effect of C_s^o is not significant compared to C_f^o. In fact, the use of this formula for the data set and spectral ranges at hand leads us to conclude that a variation as large as 400% of the self-foreign continuum coefficients, would affect the retrieval for C_f^o of less than 0.1%.

The application of the above general scheme to the retrieval of our state vector, which is composed by atmospheric and spectroscopic parameters, is not straightforward. In general if we consider one single spectrum the retrieval problem is under-constrained: we have less data than unknowns. In fact, in principle we have that the dimensionality of the spectroscopic parameters is the same as that of the data space and in addition we have the atmospheric parameters as well, hence $M < N$. Based on assumptions that will be clarified in the remaining of this section, the problem can be made over-constrained in case we co-add more spectra simultaneously for the retrieval problem. The atmospheric parameters vector is constituted by: temperature (T) and water vapour (Q) profiles, discretized over the σ-IASI atmospheric pressure levels of $N_L = 60$ layers, that is

$$\left(T_1, T_2, \ldots, T_{N_L}; Q_1, Q_2, \ldots, Q_{N_L}\right)^t \tag{9}$$

#210874 - $15.00 USD Received 24 Apr 2014; revised 7 Jun 2014; accepted 7 Jun 2014; published 1 Jul 2014

where the index t stands for transpose.

Let n be the number of spectra to be inverted, and M_R the number of spectral radiances in each single spectrum; this implies that these radiances can be written all together in a vector of length $M = M_R \times n$:

$$\mathbf{r} = \left(R_{11}, \ldots, R_{1M_R} \ldots R_{n1}, \ldots, R_{nM_R}\right)^t \tag{10}$$

The parameters to be retrieved include the n temperature and water vapour profiles, and M_R continuum coefficients, which are assumed to be the same for each spectrum and each atmospheric layer:

$$\mathbf{v} = \left(T_{11}, \ldots, T_{1N_L} \ldots T_{n1}, \ldots, T_{nN_L}; Q_{11}, \ldots, Q_{1N_L} \ldots Q_{n1}, \ldots, Q_{nN_L}; c_1, \ldots, c_{M_R}\right)^t \tag{11}$$

The assumption made for the spectroscopic coefficients means that we neglect their possible dependence on temperature and consider only the dependence on wave number. This could seem to be not consistent with theoretical calculations, e.g. [28, 29]. However, one should consider that the c-coefficients can be validly derived only at micro-window channels [11] and that ground based observations are sensitive only to the continuum emission from atmospheric layers close to the instrument. This emission occurs at a quite common *effective* temperature as shown in [11] and as further demonstrated in section 4.2 of this paper.

The appropriate Jacobian, $\mathbf{K}$ to be used in Eq. (3) has to be consistent with the structure of the state vector defined in Eq. (11) and the vector of co-added spectra as defined in Eq. (10).

To begin with, let us consider the temperature Jacobian. If $\mathbf{K}_T^{(j)}, \quad j = 1, \ldots, n$ denotes the ordinary Jacobian corresponding to the j-th spectrum (this matrix has size $M_R \times N_L$), then the appropriate Jacobian for temperature, $\mathbf{K}_T$ is obtained by considering the following block-diagonal matrix,

$$\mathbf{K}_T = \begin{pmatrix} \mathbf{K}_T^{(1)} & \mathbf{0} & \ldots & \mathbf{0} \\ \mathbf{0} & \mathbf{K}_T^{(2)} & \ldots & \mathbf{0} \\ \vdots & \vdots & \ldots & \vdots \\ \mathbf{0} & \mathbf{0} & \ldots & \mathbf{K}_T^{(n)} \end{pmatrix} \tag{12}$$

In the same way we build up the appropriate water vapour Jacobian matrix, $\mathbf{K}_Q$. Both $\mathbf{K}_T$ and $\mathbf{K}_Q$ have size $[M_R \times n] \times [N_l \times n]$.

The correct definition and computation of the Jacobian matrix for the spectroscopic coefficients is a bit more involved. For a single spectrum with M_R spectral ordinates, the Jacobian derivative for the vector of spectroscopic parameters, $\mathbf{c}$ (this vector has size M_R) has a dimension $M_R \times N_L$. Let $\mathbf{C}(i, j), i = 1, \ldots, M_R; \quad j = 1, \ldots, N_L$ be the elements of this Jacobian derivative, we have

$$C(i, j) = \frac{\partial R(i)}{\partial c(j)}; \quad i = 1, \ldots, M_r; \quad j = 1, \ldots, N_L \tag{13}$$

with $R(i)$ the radiance element corresponding to i-th channel or wave number and $c(j)$ the absorption coefficient corresponding to the j-th pressure layer. The appropriate Jacobian matrix, $\mathbf{J}_c$ to consider within the retrieval scheme with one single spectrum is the block diagonal matrix,

$$\mathbf{J}_c = \begin{pmatrix} \sum_{j=1}^{N_L} C(1, j) & 0 & \ldots & 0 \\ 0 & \sum_{j=1}^{N_L} C(2, j) & \ldots & 0 \\ \vdots & \vdots & \ldots & \vdots \\ 0 & 0 & \ldots & \sum_{j=1}^{N_L} C(M_R, j) \end{pmatrix} \tag{14}$$

Note that $\mathbf{J}_c$ has size $M_R \times M_R$.

#210874 - $15.00 USD Received 24 Apr 2014; revised 7 Jun 2014; accepted 7 Jun 2014; published 1 Jul 2014

For the retrieval problem with n co-added spectra, the Jacobian of the absorption coefficients has to be build up by piling up the n Jacobian matrices, $\mathbf{J}_c^{(i)}; \quad i = 1, \ldots, n$ (as defined in Eq. (14) in a single vertically concatenated matrix according to

$$\mathbf{K}_c = \left(\mathbf{J}_c^1, \mathbf{J}_c^2, \ldots, \mathbf{J}_c^n\right)^t \tag{15}$$

which has size $[M_R \times n] \times [M_R]$.

Having built up $\mathbf{K}_T$, $\mathbf{K}_Q$ and $\mathbf{K}_c$, we can finally compute the $\mathbf{K}$ needed to get the solution expressed by Eq. (5). This final Jacobian matrix is obtained by considering the horizontal concatenation defined by

$$\mathbf{K} = (\mathbf{K}_T, \mathbf{K}_Q, \mathbf{K}_c) \tag{16}$$

which has size $M \times N$ with $M = M_R \times n$ (the number of data points considering the n co-added spectra) and $N = 2 \times N_L \times n + M_R$ (the size of the state vector that is the number of unknowns).

We have also to define a suitable background vector and related covariance matrix before we can use the machinery of Optimal estimation as described by Eq. (5) and (6). For temperature and water vapour the background information has been derived from climatology. For this study we have used a set of radiosonde observations launched at the Dome-C site at noon of each day of the year 2012 and during the Antarctic winter of 2011. Overall, we have considered 414 radiosonde diverse profiles, including a slightly greater amount of winter profiles because of the great temperature variability in the boundary layer, that requires to be modeled accurately.

In addition to the background for (T, Q), we also need to define an appropriate background for the vector $\mathbf{c}$. The background state is obviously defined to be the MT-CKD model itself, which is our best a-priori information. For the covariance, we consider a diagonal matrix whose elements are set in order to consider a variability of 30%. This is consistent with the variability expected on the basis of previous experimental verifications of the MT-CKD model [8, 10, 11]. However, this value is further tuned and optimized because of the extra γ parameter used in our retrieval methodology.

Once we have build up the background matrices for (T, Q, c), these are combined in a block-diagonal matrix to form the final background covariance matrix, $\mathbf{S}_a$.

Finally, we need to specify the observational covariance matrix, $\mathbf{S}_\varepsilon$. This matrix ix considered to be diagonal and the elements are set equal to the squared values of the radiometric noise shown in Fig. 1. Also in this case a block-diagonal matrix has to be defined to reach consistency with the number of co-added spectra.

4. Results

For the sake of clarity, we will show the results obtained for the following cases:

- Reference case study: retrieval of atmospheric parameters alone (T, Q). This has been performed on a single-spectrum basis and using a look-up table derived from LBLRTM 12.2, AER line database 3.2, MT-CKD continuum version 2.5.2

- First case study: simultaneous retrieval of (T, Q, c). This uses the techniques of co-added spectra and the look-up table derived as before. The MT-CKD 2.5.2 continuum has been used to define the First Guess and background vectors. The derived set of continuum coefficients will be denoted by REFIR-L (the extension L refers to the LBLRTM/AER line compilation used for water vapour)

- Second case study: as item above but now the look-up table uses the HITRAN 2012 line compilation for the water vapour, and the LBLRTM 12.2 lines for the other species. Like in the previous cases, we used the MT-CKD 2.5.2 model to derive the First Guess and

#210874 - $15.00 USD Received 24 Apr 2014; revised 7 Jun 2014; accepted 7 Jun 2014; published 1 Jul 2014

background vectors, and the derived set of continuum coefficients will be denoted by REFIR-H (where the extension H is used to stress that we use the HITRAN water vapour line compilation).

4.1. *Retrieval of T, Q alone*

This case constitutes the reference situation against which we compare the spectral residual obtained with the simultaneous retrieval for (T, Q, c).

Given the fact that the water vapour precipitable amounts and the boundary layer temperature behaviours are completely different between Antarctic summer and winter, we have divided the data set according to the season in which the spectra have been acquired. We have 14 clear sky spectra for summer and 5 for the winter season. As already said in Sec. 2.3, the 14 summer spectra have been acquired during the night 9-10 February, 2012, within 5 consecutive hours of measurements (starting at 21:00 UTC). Those for the winter season on the 2nd of June 2012, from 14:00 to 18:00 UTC.

Different wave number ranges have been considered in the inversion procedure for the two data sets, essentially because the driest (winter) spectra show weaker water vapour emission lines, preventing the spectrum to saturate at wave numbers larger than 180 cm^{-1}; on the contrary, the summer spectra appear to be saturated from the water vapour emission below 240 cm^{-1}. The portion of the spectrum used in the physical retrieval has been extended until 800 cm^{-1}, excluding only the central portion of the CO_2 ν_2 emission band at 667 cm^{-1}, which again is completely saturated, and including the CO_2 feature at 791.7 cm^{-1} and some other minor water vapour lines. The portion of the spectrum above 800 cm^{-1} is left for cross check among retrieval and real observations.

The retrieval results for (T, Q) are shown in Fig. 2 and compared to the best time-space co-located ECMWF (European Centre for Medium range Weather Forecasts) analyses. For 10 February 2012 we use the analysis at 00:00 UTC, whereas for 2 June 2012 we have used the average of two analysis profiles at 12:00 UTC and 18:00 UTC. Figure 2 also shows a comparison with the two radiosonde profiles (launched at 4 UTC, noon local time) corresponding to 10 February 2012 and 2 June, respectively.

The results shown in Fig. 2 are highly consistent with the climatology of Dome-C site and show, as expected, very low amounts of water vapour and a strong temperature inversion close to the surface. It should be stressed that the retrieval is mostly sensitive to the lower atmosphere, because the Jacobian derivative shows weighting functions that peak at the surface for both temperature and water vapour. On overall, the retrieval brings poor or no information below $\approx$ 250 hPa. Figure 3 shows the observed and fitted spectra along with the spectral residual (Observations-Calculations) averaged over the 14 summer spectra. Similarly, Fig. 4 shows the results for the winter season. The overall quality of the two fits is pretty good. Both the water vapour and the temperature profiles turn out to be highly consistent with the observed spectra. The most significant discrepancy is seen for winter spectra in the core of CO_2 band, which assumes a characteristic *convex* shape induced by the strong thermal inversion near the surface. This inversion cannot be closely fitted from our procedure because of lack of vertical spatial resolution. Our pressure grid considers the first layer from 624 to 574 hPa, which corresponds to the first 600 meters above the surface, while the inversion takes place in the first 200-300 meters above the ground. However, this detail is not important to have a good quality fit of the water vapour band and no attempts were made to improve the atmospheric layering.

As a cross-check, it is noteworthy that, even though the wave numbers greater than 800 cm^{-1} have not been used in the physical retrieval procedure, the ozone band shape and intensity have been satisfactorily reproduced both in summer and winter spectra. Furthermore, it should be stressed that for ozone we use climatology and its concentration is not adjusted within the

#210874 - $15.00 USD Received 24 Apr 2014; revised 7 Jun 2014; accepted 7 Jun 2014; published 1 Jul 2014

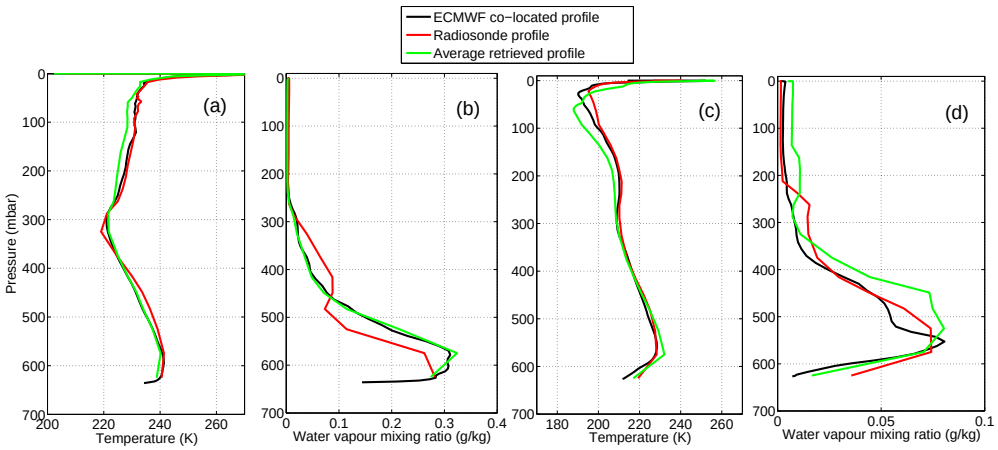

Fig. 2. (a) and (b): temperature and water vapour profiles retrieved from the analysis of the summer dataset. The retrieval has been averaged over the 14 available REFIR soundings recorded during the night of 9 January 2012 (21:00 to 2:00 UTC). The ECMWF analysis is that corresponding to 00:00 UTC, whereas the radiosonde launch is that at 04:00 UTC. (c) and (d): same as (a) and (b), but for the case of winter season. In this case the retrieval has been averaged over the 5 available REFIR soundings recorded on 2 June 2012 from 14:00 to 18:00 UTC. The ECMWF analysis is the average of the two at 12:00 and 18:00 UTC. Finally the radiosonde launch is that at 04:00 UTC.

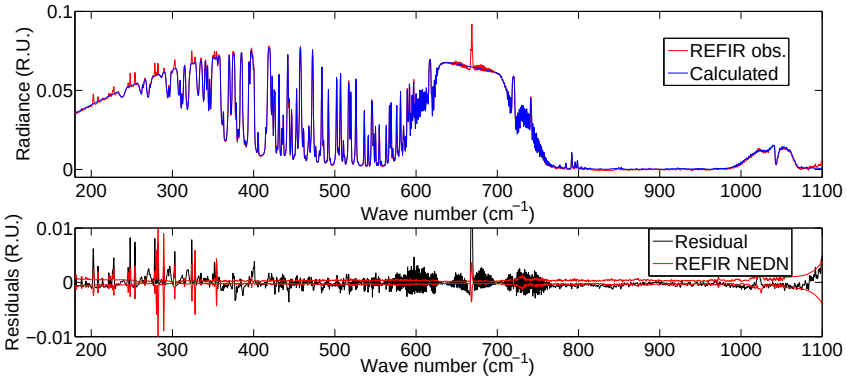

Fig. 3. Fitted and observed spectra (upper panel) and spectral residual (Bottom panel) averaged over 14 soundings. 1 R.U. = 1 W-m^{-2} sr^{-1} cm^{-1}

retrieval scheme. Thus, the good performance seen in the spectral residual at the ozone band is largely the effect of the highly consistent temperature retrieval we have obtained from the 15 μm CO_2 band.

The analysis of the water vapour rotational band fit is more complicated. The modifications of the line air-broadened halfwidths, temperature dependencies and pressure shifts in the range 350-667 cm^{-1}, introduced in the version 12.0 of LBLRTM, proved to be adequate to describe the water vapour emission [7]. On the contrary, no revisions of these parameters have been carried on in the range 12.68-350 cm^{-1}; at the same time, the MT-CKD 2.5.2 continuum version is, like the previous versions, based on an analytical form of the continuum absorption ([9],

#210874 - $15.00 USD Received 24 Apr 2014; revised 7 Jun 2014; accepted 7 Jun 2014; published 1 Jul 2014

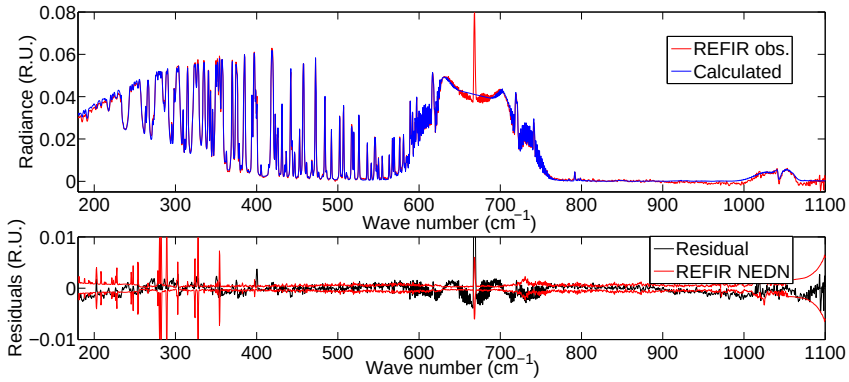

Fig. 4. As Fig. 3 but for the five spectra corresponding to the winter season. 1 R.U. = 1 W m^{-2} sr^{-1} cm^{-1}

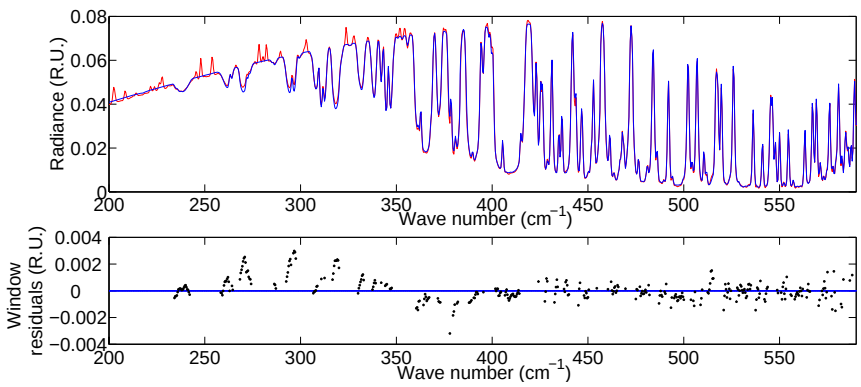

Fig. 5. Top panel: zoom of the fit in Fig. 3 showing the details of the water vapour rotational band. Bottom panel: spectral residual in the window regions. It can be seen that there is a clear slope in the residuals, which has a zero-point at 350 cm^{-1}. 1 R.U. = 1 W-m^{-2} sr^{-1} cm^{-1}

[11]). This leads to an evident misfit of the spectrum in the windows below 350 cm^{-1}.

Figure 5 shows this misfit with the residuals in the window regions below and above 350 cm^{-1}. On the one hand, the continuum model seems to be well-calibrated on the spectral lines in the range 350-590 cm^{-1}, where only minor corrections may be applied, for instance in the window around 405 cm^{-1}. On the other hand, the continuum absorption seems to be clearly underestimated below 350 cm^{-1}.

4.2. *Continuum coefficients retrieval*

As said before, we have performed two continuum coefficients retrievals. The first uses the LBLRTM 12.2 database, with the AER 3.2 line file. The coefficients have been retrieved separately for the summer and winter data sets and they will be shown for the most transparent regions of the spectrum, which can be usefully characterized as having the same effective emitting temperature:

$$T_{eff}(i) = \frac{\sum_{j=1}^{N_L} |C_{ij}| T_j}{\sum_{j=1}^{N_L} |C_{ij}|} \tag{17}$$

where $|C_{ij}|$ is the absolute value of the Jacobian calculated with respect to the continuum co-

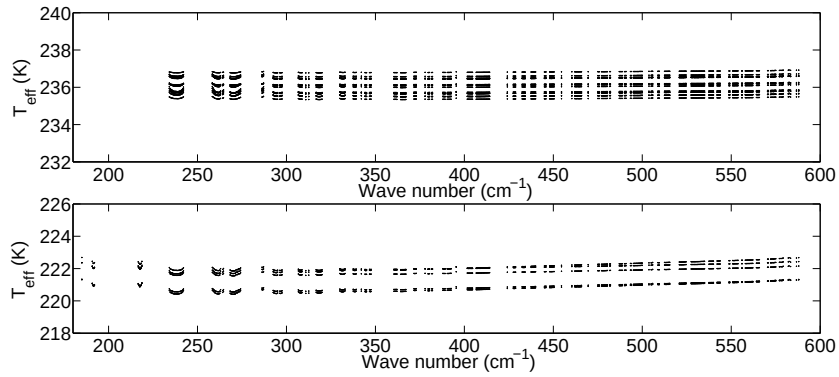

Fig. 6. Effective emitting temperature for the spectra selected for the continuum coefficients retrieval. Top panel: summer spectra; bottom panel: winter spectra.

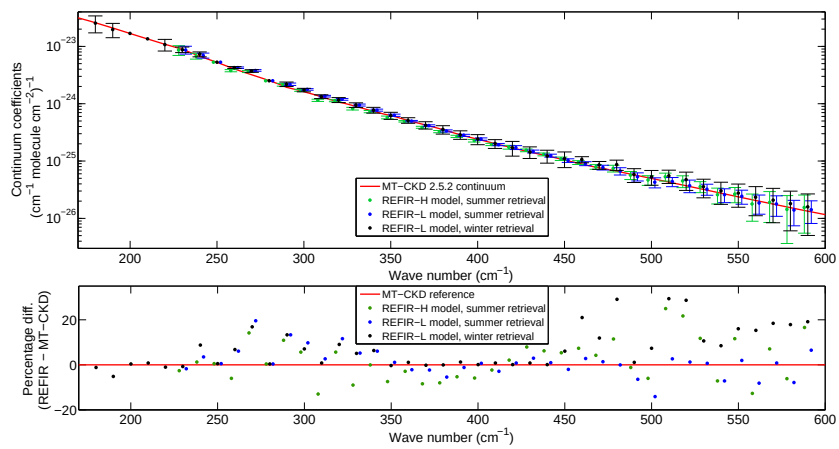

Fig. 7. Retrieved continuum coefficients using the two data sets and the two different line compilations considered in this work (tabulated values are available on request from the authors).

efficient at the wave number σ_i, and at the j-th layer, and T_j being the temperature of the j-th layer. For a single spectrum, the window channels of the water vapour rotational band tend to have the same value of T_{eff}, because the instrument is usually sensitive to the continuum emission of the atmospheric layers close to the instrument itself. Moreover, the retrieved continuum coefficients are referred to a particular value of T_{eff}, so the spectra to be used in the procedure must be chosen in such a way that their values of T_{eff} are similar. With this criterion, we have chosen the 14 summer spectra and the 5 winter ones, whose T_{eff} was within a range of ± 2 K. Figure 6 shows the values of T_{eff} in the window channels.

On overall, the water vapour and temperature profiles are vectors made up by 42 values for each spectrum, while the number of continuum coefficients is the same of the spectral channels used in the retrieval; in the case of the summer data set, we work with 1179 spectral channels for each spectrum, so we have 1179$\times$14=16506 independent pieces of information, while the number of parameters to retrieve is (42$\times$2)$\times$14+1179=2355; in the case of the winter data set, making the same check, we have 5895 spectral points against 1599 parameters. The continuum

#210874 - $15.00 USD Received 24 Apr 2014; revised 7 Jun 2014; accepted 7 Jun 2014; published 1 Jul 2014

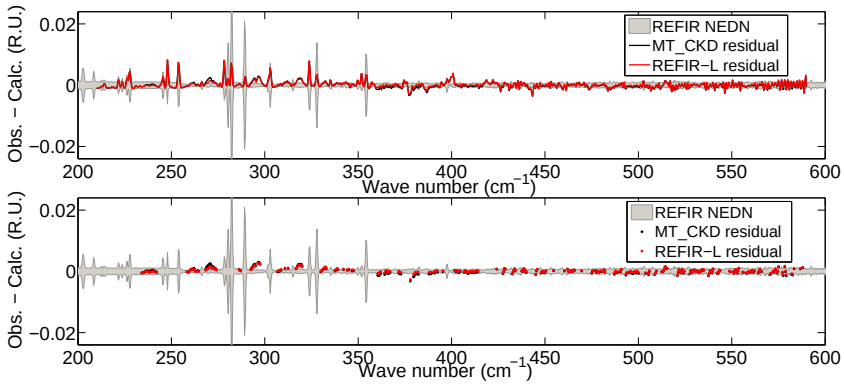

Fig. 8. Spectral residual comparison using the two continuum models on the same set of summer spectra presented in Fig. 3. Top panel shows the complete residuals, bottom panel only those in the window channels. 1 R.U. = 1 W-m^{-2} sr^{-1} cm^{-1}

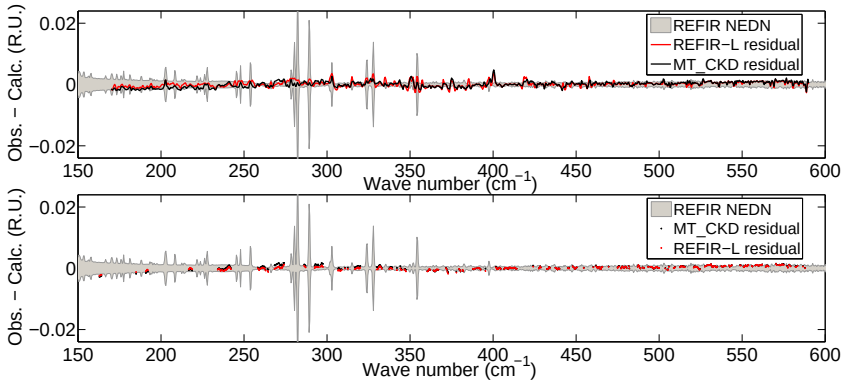

Fig. 9. Same as in Fig. 8, but for the winter data set. 1 R.U. = 1 W-m^{-2} sr^{-1} cm^{-1}

coefficients retrieved with the LBLRTM/AER absorption line database are consistent with the spectral residual shown in the previous section (Fig. 3- 4) Below 350 cm^{-1}, to compensate for the negative (downward) bias in the spectral residual, the retrieved continuum coefficients tend to be greater than those of MT-CKD model.

It should be stressed that at wave numbers where the water vapour line absorption dominates over that of the continuum component, we have no information about the corresponding *c*-values. To avoid useless complications, at wave numbers dominated by line absorption, the *c*-Jacobian is set to zero and the retrieval relaxes to the background, that is the MT-CKD model. At the end of the retrieval procedure, the retrieved continuum coefficients have been binned at a resolution of 10 cm^{-1}. The continuum coefficients obtained for the two data sets, summer and winter, are shown in Fig. 7. The error bars assigned to the continuum coefficients have been consistently derived from the physical retrieval procedure, through the calculation of the a-posteriori covariance matrix of Eq. (6).

The results in the range 350-590 cm^{-1}, instead, are consistent with the MT-CKD model, apart from minor discrepancies in the wide spectral window around 405 cm^{-1}. What is interesting to stress, is that the REFIR-L coefficients obtained using the summer and the winter data set are largely consistent. The above conclusion is also obtained by looking at the spectral residuals, which are shown in Fig. 8 for the summer data set and Fig. 9 for the winter data set.

#210874 - $15.00 USD Received 24 Apr 2014; revised 7 Jun 2014; accepted 7 Jun 2014; published 1 Jul 2014

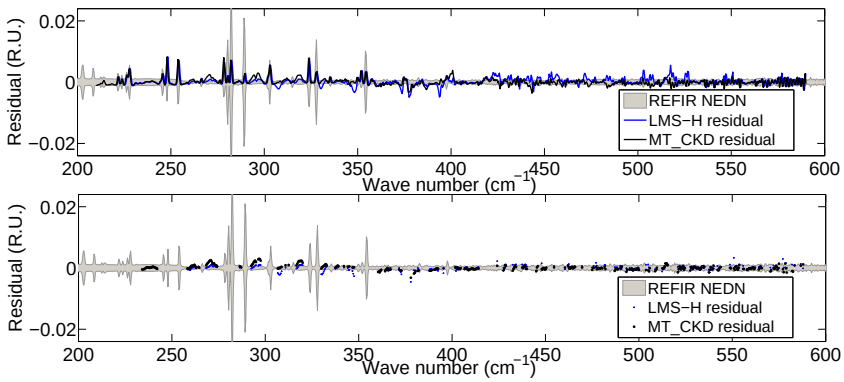

Fig. 10. Fit residuals using the LMS-H continuum and the HITRAN lines on the summer data set. 1 R.U. = 1 W-m^{-2} sr^{-1} cm^{-1}

The comparison provided in Fig. 8-9 makes clear how our REFIR-L coefficients enhance the overall retrieval performance throughout the interval interested by the water vapour rotational band with respect to the MT-CKD continuum. The improvement of the spectral quality is even more significant in the window channels, where the continuum contribution should be dominant; our fitted continuum yields better performance than MT-CKD in both data sets. However, it should be stressed that these improvements are normally within error bars, which means that the MT-CKD model does perform well and we cannot see dramatic differences between model and retrieval. Moreover, discrepancies which exceed error bars are more likely to occur in regions of the spectrum which are dominated by line absorption. This effect is much more evident below 350 cm^{-1}, which exemplifies the need of a revision of the line contribution, much more than that of continuum.

This conclusion is much more reinforced with the second retrieval exercise, where we use the HITRAN water vapour line compilation, instead of that provided by LBLRTM/AER. The reason for this exercise is just to analyze how much important the adjustment of line parameters performed with the compilation LBLRTM/AER is. Is this adjustment crucial to perform a good fit of observations within the range 350 to 600 cm^{-1}?

To address this issue, we have performed this second retrieval exercise, where the first guess and background for the continuum coefficients is again the MT-CKD model, but now the line compilation is that of HITRAN. For the sake of brevity, this exercise has been limited to the summer data set alone. The retrieved *c*-coefficients are shown in Fig. 7. It should be stressed that these coefficients cannot be straightforwardly compared to those provided by the MT-CKD model, since they correspond to different line compilations. REFIR-L may be compared to MT-CKD, however, with respect to REFIR-H, MT-CKD has to be intended just as a reference.

Nevertheless, the fact that REFIR-H coefficients are significantly lower than the REFIR-L and MT-CKD ones, is consistent with the halfwidths reduction considered in the LBLRTM/AER data set; the result is that more continuum contribution is needed to produce the same optical depth as that yielded by the HITRAN database, but with a lower continuum component.

If we look at the spectral residuals in Fig. 10, we see that the REFIR-H approach allows us to reduce most of the difference between observations and calculations within the error bars. However, in comparison to the reference MT-CKD, the spectral residual (line+continuum) has a larger bias and variability, especially in the spectral region above 350 cm^{-1}. This is also evident in case we perform a direct computation of bias and standard deviation of the spectral residual. This computation is shown in Table 2 both for the case of lines+continuum and for the

#210874 - $15.00 USD Received 24 Apr 2014; revised 7 Jun 2014; accepted 7 Jun 2014; published 1 Jul 2014

case of window regions, where the effect of continuum absorption dominates. In conclusion, it

Table 2. Upper table: mean of the absolute values of residuals and their standard deviation for the range 180-590 cm^{-1} for the three combinations spectral database+continuum treated in this case. Lower table: Same as upper, but the calculation has been done only considering the window channels. Values are provided in Radiance Units (1 R.U.=1 W-m^{-2} sr^{-1} cm^{-1}) divided by 1000, so a value of 1 is equivalent to 1 mW m^{-2} sr^{-1} cm.

data set	Line database + continuum	Average abs. residual	Residuals Std. Dev.
Summer	LBLRTM + MT-CKD 2.5.2	0.81	0.61
	LBLRTM + REFIR-L	0.75	0.60
	HITRAN + REFIR-H	0.90	0.64
Winter	LBLRTM + MT-CKD 2.5.2	0.73	0.54
	LBLRTM + REFIR-L	0.65	0.53

data set	Line database + continuum	Average abs. residual	Residuals Std. Dev.
Summer	LBLRTM + MT-CKD 2.5.2	0.58	0.48
	LBLRTM + REFIR-L	0.48	0.61
	HITRAN + REFIR-H	0.52	0.58
Winter	LBLRTM + MT-CKD 2.5.2	0.58	0.54
	LBLRTM + REFIR-L	0.47	0.55

seems that the adjustment of line half-widths performed with the compilation LBLRTM/AER has its validity and most of the improvement in fitting observations seems to be the result of line adjustment rather than better continuum absorption modeling.

4.3. Retrieval sensitivity

In this section we compare the two (T,Q) products obtained with and without the simultaneous retrieval of water vapour continuum absorption coefficients. This very simple exercise allows to asses the sensitivity of (T,Q) to the continuum change we have evidenced in the analysis.

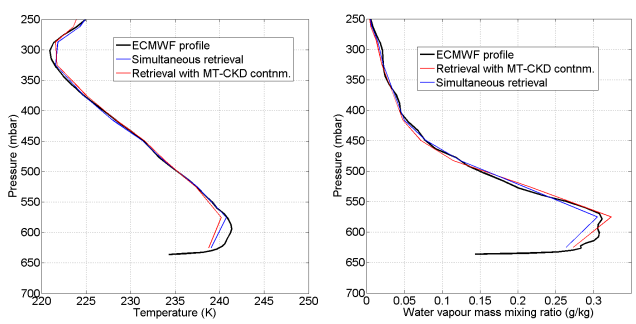

Fig. 11. Comparison between the average temperature (left) and water vapour (right) profiles obtained with the simultaneous and non-simultaneous retrieval.

The comparison is provided in Fig. 11, where we also show the time space co-located ECMWF analysis. As already stressed also in section 4.1, a sensitivity analysis performed with the Jacobian derivative shows that the spectral radiance is sensitive to (T,Q) mostly in the pressure range from the ground level to $\approx$ 250 hPa. Therefore the comparison is limited to that pressure

range. The results show that the retrieval captures the salient characteristics of both temperature and water vapour vertical structures in the lower atmosphere. The other and most important feature of this comparison is that the two retrievals do not show important difference each from other. Differences are mostly seen in the boundary layer, but they are not as dramatic as to evidence a high sensitivity of (T,Q) retrieval to the water vapour continuum coefficients change. In other words, the change of the continuum absorption seems to have little or no important effect over the retrieval.

5. Conclusions

We have developed a novel methodology to simultaneously retrieve atmospheric and spectroscopic parameters. The methodology relies on Optimal Estimation as far as the retrieval aspects are concerned and suitable forward calculations, which in turn make use of a radiative transfer model capable of computing analytical Jacobian derivatives for atmospheric parameters, such as temperature and humidity, and spectroscopic parameters, such as water vapour continuum absorption. The new methodology makes less critical the need of an independent characterization of the thermodynamical state of the atmosphere (e.g. with co-located radiosonde observations), because this state is consistently and simultaneously derived from the spectral radiances themselves. In addition, the process eliminates the need of somewhat ad hoc adjustments of the temperature and humidity profiles, while reducing possible biases because of uncertainty about the atmospheric state.

Using REFIR observations acquired at the Antarctica Dome-C site, the methodology has been used to check the consistency and quality of the MT-CKD continuum model within the spectral range 180 to 600 cm^{-1} which encompasses the fundamental water vapour rotational band.

Two sets of basic retrieval have been performed. The first one uses LBLRTM 12.2, AER line database 3.2 along with the MT-CKD continuum version 2.5.2 as the first guess and background. This retrieval exercise has allowed us to assess the good performance of the MT-CKD model.

With the objective of getting a better insight into understanding whether or not AER line database 3.2 improves over the current HITRAN version, we have found that there is experimental evidence for the AER line compilation. This evidence justifies the need of adjusting the water vapour line half widths in the spectral range 350 to 600 cm^{-1}. Also there is further experimental evidence that a similar adjustment is needed also in the range below 350 cm^{-1}, where we have observed the larger misfit between observations and calculations.

To sum up, we conclude that this new set of Antarctica Dome-C REFIR observations definitely validates the current MT-CKD 2.5.2 model parameterization, even if our results do show that further improvements are possible and the need to strengthen the lines, rather than continuum, parameterization in the range below 350 cm^{-1}. These improvements are both of interest to spectroscopy itself, and applications to the study of climate processes and related feedback on radiative forcing.

Acknowledgments

Work supported by Programma Nazionale di Ricerche in Antartide (P.N.R.A.). Radiosonde data were obtained from www.climantartide.it